4.7 SST PERTURBATION EXPERIMENTS IN THE CSU GENERAL CIRCULATION MODEL: IMPACT ON SIMULATED CLOUD TYPES

Laura D. Fowler* and David A. Randall
Colorado State University, Fort Collins, Colorado

1. INTRODUCTION

During the last decade or so, little progress has been made in our understanding of the response of upper-tropospheric cloudiness in climate change experiments simulated with general circulation models (GCMs), as concluded by the Intergovernmental Panel on Climate Change (IPCC) Third Assessment Report (2001). This lack of progress results, in part, because GCMs have difficulties to simultaneously simulate the global vertical distributions of cloudiness and its optical properties, hence producing a wide range of cloud feedback parameters in response to ±2K sea-surface temperature (SST) perturbations, as discussed by Cess et al. (1990; 1996).

Earlier GCM studies show that, when SSTs increase, low-level cloudiness decreases and high-level cloudiness increases. The change in the vertical distribution of clouds yields a positive feedback through the enhanced greenhouse effect of upper-tropospheric clouds, further increasing the surface warming (Schlesinger and Mitchell 1987; Wetherald and Manabe 1988). GCM sensitivity analyses also show that the magnitude of this positive cloud feedback can be dampened, or become negative, depending on the complexity of parameterized cloud microphysical processes and precipitation, and cloud optical properties (Le Treut and Li 1991; Mitchell et al. 1989, Roeckner et al. 1987).

In this study, we repeat the ±2K SST perturbation experiment, first proposed by Cess and Potter (1988) as a surrogate climate change scenario, using the Colorado State University (CSU) GCM. We focus our analysis on the combined variations in the amount and optical properties of upper-tropospheric clouds when SSTs increase.

2. THE CSU GCM

In the recent years, parameterized dynamical and physical processes in the CSU GCM have been considerably improved.

The CSU GCM uses a new type of dynamical core which solves the vorticity and divergence equations in place of the momentum equations (Ringler et al. 2000). A unique feature of the new dynamical core is that the model is discretized in the horizontal on a geodesic grid that is nearly uniform over the entire globe, as discussed in Heikes and Randall (1995a; 1995b). The vertical discretization is based on a modified σ coordinate system in which the planetary boundary layer (PBL) is prognostic and fills the bottom layer of the model (Suarez et al. 1983).

Convection is simulated using the parameterization of Fowler and Randall (2002), as proposed by Arakawa and Schubert (1974). Convection is allowed to start at each model level starting from the top of the PBL. Large-scale water vapor, cloud water, and cloud ice are entrained at the bottom and sides of the convective updrafts while in-cloud water, cloud ice, and snow are detrained at cloud-tops. Inside convective clouds, microphysical processes are calculated for the water and ice phase, separately. Cloud water and cloud ice are allowed to coexist inside a prescribed but easily adjustable temperature range. All convective rain formed by auto conversion of in-cloud cloud water falls to the surface instantaneously. All or a fraction of the convective snow formed by auto conversion of in-cloud cloud ice can be detrained at cloud-tops while the remaining fraction is added to the convective rain. The parameterization of large-scale saturation clouds uses the bulk cloud microphysics scheme developed by Fowler et al. (1996), and is based on the mesoscale cloud models developed by Lin et al. (1983) for the cold phase, and Rutledge and Hobbs (1983; 1984) for the warm phase.

The narrow-band parameterization of long and short wave radiation follows Stephens et al. (2001). The infrared and solar spectra are divided into 12 and 6 spectral intervals, respectively. In each spectral interval, non-gray gaseous absorption by H_2O, CO_2, O_3, CH_4, and N_2O are calculated using correlated k-distributions following Fu and Liou (1992). Spectral optical properties of water, ice, and mixed-phase clouds are computed using the anomalous diffraction theory, as described in Stephens et al. (1990). Cloudy and cloud-free long and short wave fluxes are obtained using a delta two-stream approximation.

3. SST PERTURBATION EXPERIMENTS

The control (CTRL) experiment, and +2K (SSTp2) and -2K (SSTm2) perturbation experiments of the sea-surface temperature (SST) were run for perpetual July conditions with fixed soil moisture, following the procedure proposed by Cess and Potter (1988). Each simulation was run for 180 days and results are discussed using the last 30-day mean.

To compare the global distribution of clouds simulated with the CSU GCM against ISCCP data, we used an algorithm known as the "ISCCP simulator", first proposed by Yu et al. (1986), and further developed and made widely available to the community by Dr. S. Klein (Klein and Jakob 1999) and Dr. M. Webb (Webb et al. 2001). In a nutshell, the ISCCP simulator emulates the ISCCP retrieval using the vertical distributions of cloud amounts and cloud optical properties, and atmospheric profiles simulated by GCMs. The ISCCP simulator outputs the frequencies of occurrence of clouds as func-

* *Corresponding Author address*: Laura D. Fowler, Colorado State University, Dept. of Atmospheric Science, Fort Collins, CO 80523-1371; e-mail: laura@atmos.colostate.edu.

tions of cloud optical thickness (τ) and cloud-top pressure, as defined by the ISCCP radiometric cloud classification (Rossow and Schiffer 1991).

In the following section, we focus our results on the geographical distributions of high-level clouds (defined as clouds with cloud-top pressures less than 440 hPa) in terms of cirrus, cirrostratus, and deep convective clouds. Deep convective clouds are the optically thickest upper-tropospheric clouds, associated with the coldest cloud-top temperatures. Cirrostratus are cloud anvils formed by detrainment at the tops of narrow convective updrafts. Finally, tropical cirrus are optically thin clouds that can be thought as convective cloud debris that are advected away from convective sources by the large-scale flow.

4. RESULTS

Comparing the July geographical distributions of simulated cirrus, cirrostratus, and deep convective clouds against ISCCP data reveals significant differences between the model and observations. As a whole, the CSU GCM strongly overestimates the amount of high-level clouds, and simulated clouds are optically too thin relative to the observations, especially in the tropics. As seen in Fig. 1, simulated cirrus are significantly underestimated along the Inter-Tropical Convergence Zone (ITCZ) and the warm pool region over the oceans, as well over land in the Northern Hemisphere, when compared against ISCCP data. As simulated cirrus, cirrostratus are also strongly underestimated in the tropics over land and oceans, and strongly overestimated at high latitudes (not shown). Figure 2 shows that the GCM has difficulties simulated optically thick upper-tropospheric clouds. In the tropics, the GCM reproduces relatively well deep convective clouds along the ITCZ and the warm pool regions. At high latitudes, the GCM is shown to simulate a lot of deep convective clouds, as labelled by the ISCCP simulator, especially in the Summer Hemisphere. It is important to note that these optically thick upper-tropospheric clouds were actually formed through large-scale condensation processes, and not by convective detrainment.

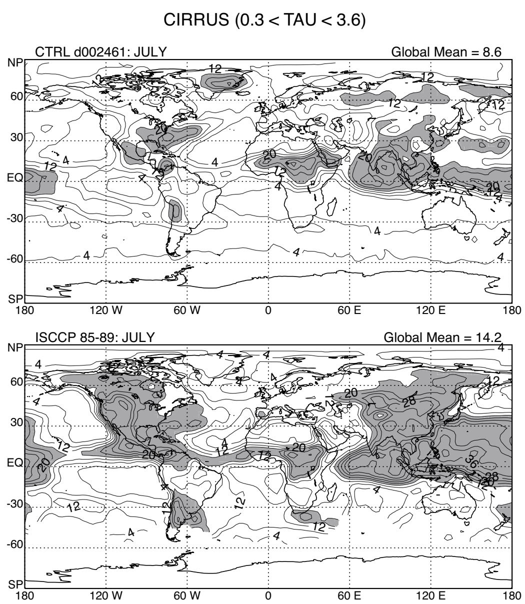

FIGURE 1. July geographical distributions of cirrus simulated with the CSU GCM in the CTRL experiment (top panel), and from ISCCP data (bottom panel). Units are percent, and dark shading corresponds to cirrus amounts greater than 16%.

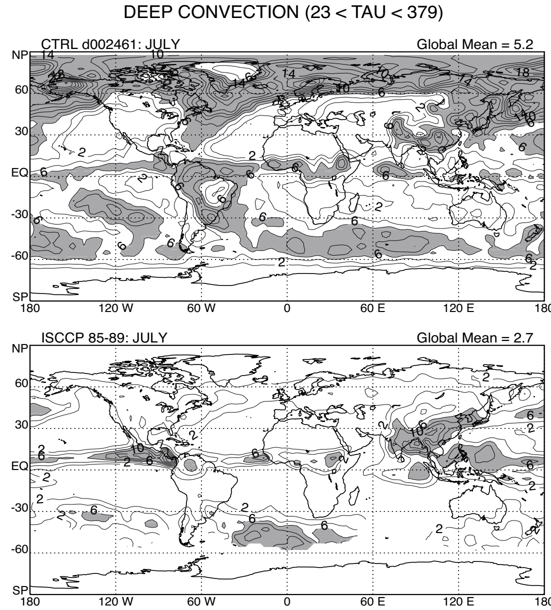

FIGURE 2. July geographical distributions of deep convective clouds simulated with the CSU GCM in the CTRL experiment (top panel), and from ISCCP data (bottom panel). Units are percent, and dark shading corresponds to deep convective cloud amounts greater than 6%.

Uniformly increasing SSTs leads to enhanced convective activity over the oceans, hence producing more upper-tropospheric clouds through convective detrainment, a mechanism already discussed in earlier studies (Le Treut and Li. 1991; Mitchell et al. 1989). However, the increase in high-level cloudiness is not uniform, and is modulated by accompanying variations in its optical properties. Figure 3 displays the July geographical distributions of the difference in cirrus, cirrostratus, and deep convective clouds between SSTp2 and SSTm2. The SSTp2 minus SSTm2 differences in cirrostratus and deep convective clouds are very small in the tropics, i.e. over areas where their mean cloud amounts are simulated to be too small (refer to Fig. 2). In contrast, differences in both cloud types are large at high latitudes where their mean cloud amounts are simulated to be too large relative to the ISCCP data. SSTp2 minus SSTm2 differences in cirrus are geographically more organized than for optically thicker high-level clouds. The amount of cirrus is shown to increase in the eastern Pacific and the middle latitude storm track regions. Optically thin clouds are simulated to decrease over the western Pacific and tropical land masses. Because of the large discrepancies between the simulated and observed global distributions of high-level cloud types, it is difficult to relate, at least at this stage, their SSTP2 minus SSTm2 differences to actual cloud feedbacks.

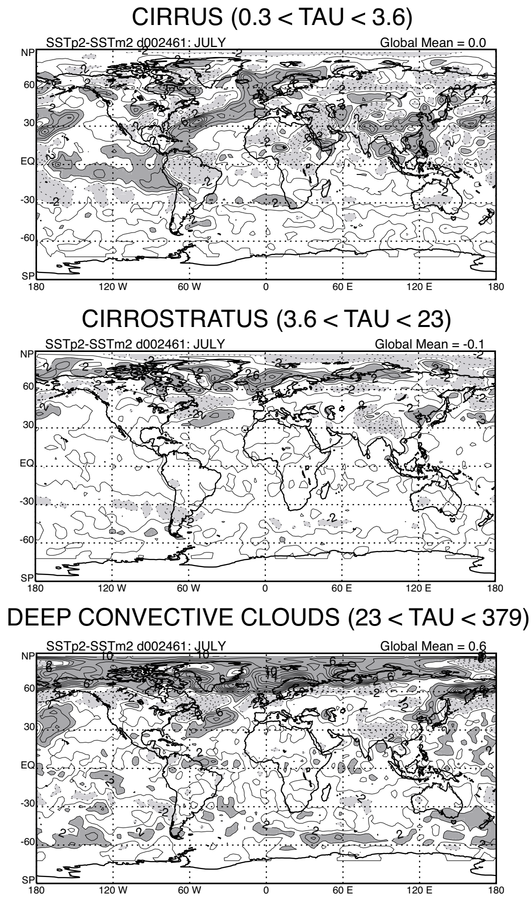

FIGURE 3. July geographical distributions of the difference in cirrus (top panel), cirrostratus (middle panel), and deep convective clouds (bottom panel) between the SSTp2 and SSTm2 experiments. Units are percent. Light shading corresponds to differences less than -2% and dark shading correspond to differences greater than 2%.

5. SUMMARY AND CONCLUSIONS

In this study, we started to investigate how upper-tropospheric clouds respond to increasing SSTs. In particular, we sought to use the ISCCP simulator to distinguish between the response of optically thin and thicker clouds, following the ISCCP radiometric cloud classification. Results from the CTRL experiment suggest that we first need to improve the simulated distributions of cirrus, cirrostratus, and deep convective clouds. In the tropics, it is most likely that the limited response of thick clouds results because of deficiencies in the parameterized physics, and not because of real physical processes. However, this issue remains to be investigated as well. Using the ISCCP simulator to decipher cloud feedback mechanisms as functions of cloud types is a tool that can be successfully use to separate the cloud feedback due to the change in the vertical distribution of clouds to that due to the change in the optical properties of cloudiness.

6. ACKNOWLEDGMENTS

The authors thank Drs. S. Klein and M. Webb for providing the source code of the ISCCP simulator, and their comments on how to best use the simulator with the CSU GCM. This research is sponsored by the National Science Foundation under grant ATM-9812384 and the Department of Energy under grant DE-FG03-02ER63323.

7. REFERENCES

Arakawa, A., and W. H. Schubert, 1974: Interactions of a cumulus cloud ensemble with the large-scale environment. Part I: *J. Atmos. Sci.*, **31**, 674-701.

Cess, R.D., and G.L. Potter, 1988: A methodology for understanding and intercomparing atmospheric climate feedback processes in general circulation models. *J. Geophys. Res.*, **93**, NO. D7, 8305-8314.

Cess, R.D., and authors, 1990: Intercomparison and interpretation of climate feedback processes in 19 atmospheric general circulation models. *J. Geophys. Res.*, **95**, 16,601-16,615.

Cess, R.D., and authors, 1996: Cloud feedback in atmospheric general circulation models: An update. *J. Geophys. Res.*, **101**, 12,791-12,794.

Fowler, L. D., and D. A. Randall, 2002: Interactions between cloud microphysics and cumulus convection in a general circulation model. *J. Atmos. Sci.*, **59**, 3074-3098.

Fowler, L. D., D. A. Randall, and S. A. Rutledge, 1996: Liquid and ice cloud microphysics in the CSU General Circulation Model. Part I: Model description and simulated cloud microphysical processes. *J. Climate*, **9**, 489-529.

Fu, Q., and K. N. Liou, 1992: On the correlated k-distribution method for radiative transfer in nonhomogeneous atmospheres. *J. Atmos. Sci.*, **49**, 2139-2156.

Heikes, R., and D. A. Randall, 1995a: Numerical integration of the shallow-water equations on a twisted icosahedral grid. Part I: Basic design and results of tests. *Mon. Wea. Rev.*, **123**, 1862-1880.

Heikes, R., and D. A. Randall, 1995b: Numerical integration of the shallow-water equations on a twisted icosahedral grid. Part II: A detailed description of the grid and an analysis of numerical accurary. *Mon. Wea. Rev.*, **123**, 1881-1887.

Klein, S.A., and C. Jakob, 1999: Validation and sensitivities of frontal clouds simulated by the ECMWF model. *Mon. Wea. Rev.*, **127**, 3514-2531.

Le Treut, H., and Z-X. Li, 1991: Sensitivity of an atmospheric general circulation model to prescribed SST change: feedback effects associated with the simulation of cloud optical properties. *Clim. Dyn.*, **5**, 175-187.

Lin, Y.-L., R. D. Farley, and H. D. Horville, 1983: Bulk parameterization of the snow field in a cloud model. *J. Climate Appl. Meteor.*, **22**, 1065-1092.

Mitchell, J.F.B., C.A. Senior, and W.J. Ingram, 1989: CO_2 and climate: A missing feedback? *Nature*, **341**, 132-134.

Ringler, T.D., R. Heikes, and D.A. Randall, 2000: Modeling the atmospheric general circulation using spherical geodesic grids: A new class of dynamical cores. *Mon. Wea. Rev.*, **128**, 2471-2490.

Rossow, W.B., and R.A. Schiffer, 1991: ISCCP cloud data products. *Bull. Amer. Meteor. Soc.*, **72**, 2-20.

Rutledge, S. A., and P. V. Hobbs, 1983: The mesoscale and microscale structure and organization of clouds and precipitation in midlatitude cyclones. VIII: A model for the "seeder-feder" process in warm-frontal rainbands. *J. Atmos. Sci.*, **40**, 1185-1206.

Roeckner, E., U. Schlese, J. Biercamp, and P. Loewe, 1987: Cloud optical depth feedbacks and climate modelling. *Nature,* **329**, 138-140.

Rutledge, S. A., and P. V. Hobbs, 1984: The mesoscale and microscale structure and organization of clouds and precipitation in midlatitude cyclones. XII: A diagnostic modeling study of precipitation development in narrow cold-frontal rainbands. *J. Atmos. Sci.*, **41**, 2949-2972.

Schlesinger, M.E., and J.F.B. Mitchell, 1987: Climate model simulations of the equilibrium climatic response to increased carbon dioxide. *Rev. Geophys.*, **25**, 760-798.

Stephens, G. L., P. M. Gabriel, and P. T. Partain, 2001: Parameterization of atmospheric radiative transfer. Part I: Validity of simple models. *J. Atmos. Sci.*, **58**, 3391-3409.

Stephens, G. L., S.-C. Tsay, P. W. Stackhouse, Jr., and P. J. Flatau, 1990: The relevance of microphysical and radiative properties of cirrus clouds to climate and climatic feedbacks. *J. Atmos. Sci.*, **47**, 1742-1753.

Suarez, M.J., A. Arakawa, and D.A. Randall, 1983: Parameterization of the planetary boundary layer in the UCLA general circulation model: Formulation and results. *Mon. Wea. Rev.*, **111**, 2224-2243.

Webb, M., C. Senior, S. Bony, and J.-J. Morcrette, 2001: Combining ERBE and ISCCP data to assess clouds in the Hadley Centre, ECMWF, and LMD atmospheric climate models. *Clim. Dyn.*, **17**, 905-922.

Wetherald, R.T., and S. Manabe, 1988: Cloud feedback processes in a general circulation model. *J. Atmos. Sci.*, **45**, 1397-1415.

Yu W., M. Doutriaux, G. Seze, H. Le Treut, and M. Desbois, 1996: A methodology study of the validation of clouds in GCMs using ISCCP satellite observations. *Clim. Dyn*., **12**, 389-401.